Published in final edited form as:
Science. 2013 October 4; 342(6154): 111–114. doi:10.1126/science.1236921.

Allele-specific Silencing of Mutant *Myh6* Allele in Mice Suppresses Hypertrophic Cardiomyopathy

Jianming Jiang[1,3,4,*], **Hiroko Wakimoto**[1,2,3,*], **J. G. Seidman**[1,†], and **Christine E. Seidman**[1,3,4,†]

[1]Department of Genetics, Harvard Medical School, Boston, MA 02115, USA

[2]Department of Cardiology, Children's Hospital Boston, Boston, Massachusetts, USA

[3]Division of Cardiovascular Medicine, Brigham and Women's Hospital, Boston, Massachusetts, USA

[4]Howard Hughes Medical Institute, Boston, Massachusetts, USA

Abstract

Dominant mutations in sarcomere proteins such as the myosin heavy chains (MHC) are the leading genetic causes of human hypertrophic cardiomyopathy (HCM) and dilated cardiomyopathy (DCM). Here we demonstrate that expression of the HCM cardiac MHC gene *(Myh6)* R403Q mutation in mice can be selectively silenced by an RNAi cassette delivered by an adeno-associated virus vector. RNAi-transduced $MHC^{403/+}$ mice had neither hypertrophy or myocardial fibrosis, the pathologic manifestations of HCM for at least 6 months. As inhibition of HCM was achieved by only a 25% reduction in the levels of the mutant transcripts, we suggest that the variable clinical phenotype in HCM patients reflects allelic-specific expression and that partial silencing of mutant transcripts may have therapeutic benefit.

Hypertrophic cardiomyopathy (HCM) is an autosomal dominant disease characterized by an increase in left ventricular wall thickness (LVWT), disorganization of cardiomyocytes and expansion of myocardial fibrosis that occurs in the absence of systemic disease (1–3). HCM is the leading cause of non-violent sudden death in young adults and the most common cause of sudden death on the athletic field(4). HCM is caused by mutations in genes that encode protein constituents of the cardiac sarcomere, the contractile unit of muscle (5, 6) More than 1000 distinct pathogenic mutations have been identified, and over half of these occur in *MYH7* (encoding β myosin heavy chain) and *MYBPC* (encoding myosin binding protein-C)(7). Most HCM mutations, and all that occur in *MYH7*, are missense mutations, producing amino acid substitutions in myosin that perturb the sarcomere's contractile function.

The human HCM mutation *MYH7* R403Q causes particularly severe disease that is characterized by early-onset and progressive myocardial dysfunction, and a high incidence of sudden cardiac death (8). Heterozygous $MHC^{403/+}$ mice express the R403Q mutation in

To whom correspondence should be addressed. cseidman@genetics.med.harvard.edu.
*,†Contributed equally to this work

Myh6, under the control of the endogenous *Myh* locus. *Myh6* and *MYH7* are highly homologous in sequence and encode the predominant myosin isoforms in the adult hearts. $MHC^{403/+}$ mice recapitulate human HCM and develop hypertrophy, myocyte disarray and increased myocardial fibrosis (9). Analyses of mutant myosins isolated from $MHC^{403/+}$ mice showed that HCM mutations cause fundamental changes in sarcomere functions, including increased acto-myosin sliding velocity, force generation, and ATP hydrolysis (10). These changes in turn alter calcium cycling and gene transcription in myocytes and ultimately induce pathologic remodeling of the heart *in vivo* (11, 12,13). Understanding this pathogenic cascade has led to the identification of secondary signaling molecules as potential therapeutic targets (13,14), but no strategies have been defined that correct the primary biophysical and biochemical abnormalities of sarcomeres with HCM mutations.

Selective reduction in the expression of the mutant protein would be the most direct approach for correcting sarcomere dysfunction. As a first step in pursuing this strategy, we determined whether *in vivo* allele-specific repression of *Myh6* R403Q was feasible. Because mice hemizygous for a normal *Myh6* gene are viable, fertile, and have essentially normal cardiac function (15), we reasoned that inactivation of the mutant sarcomere protein allele is unlikely to have adverse cardiovascular effects. We used an RNA interference (RNAi) construct because this powerful tool has successfully reduced gene expression in many systems and can distinguish between genes that differ by one single nucleotide (16). We selected adeno-associated virus packed with serotype 9 capsid (AAV-9) as a delivery vehicle because this vector has strong tropism for cardiac tissues (17,18). To enhance the cardiac tropism we engineered the vector so that AAV-9 expression was under the control of the cardiac specific troponin T (cTnT) promoter.

We produced 17 unique RNAi constructs, co-transfected each with a plasmid carrying the *Myh6* R403Q mutant gene into 293T human embryonic kidney cells (fig.S1a). One RNAi construct, designated 403m, significantly reduced *Myh6* R403Q expression (Fig. 1A, B). To assess its specificity, we transfected wild-type or mutant *Myh6* into 293T cells with 403m constructs. Because there was significant silencing (~80%) of both wild-type and mutant *Myh6* expression, we introduced an additional mismatch into the 403m RNAi construct (designated 403i; Fig. 1A). 403i had modest reduction (~20%) of wild-type *Myh6* expression, but retained approximately 80% reduction in the expression of *Myh6* R403Q transcript in 293T cells (Fig. 1B).

To ascertain the cardiac selectivity of AAV-9-cTnT vector, we used enhanced green fluorescent protein (EGFP) (fig.S1b). Virus was injected (5×10^{13} vector genomes (vg)/kg) into the thoracic cavity of one-day old mice (Supplementary Methods) and after 3 weeks, all organs were dissected and EGFP expression was assessed by fluorescence microscopy. EGFP expression occurred exclusively in the heart and was absent in other organs including the brain, lung and spleen (fig. S2). EGFP expression was present within 48 hours after virus transduction and remained robust for 12 months (fig. S2, 3).

We next engineered 403i shRNA or control shRNA (denoted 403i RNAi and control RNAi, respectively) into the AAV-9-cTnT-EGFP-RNAi vector so that all cells expressing EGFP would also express shRNAs. To assess the efficacy of 403i shRNA *in vivo*, we injected

variable amounts of 403i RNAi-encoding viruses (5×10^{9}, 5×10^{11} and 5×10^{13} vg/kg) into the thoracic cavity of one-day old mice. Two weeks after viral transduction, total RNA extracted from each left ventricle (LV) was individually analyzed by RNA-seq(19). Sequencing reads that corresponded to *Myh6* R403Q or wild-type *Myh6* were counted and visualized using Integrative Genomics Viewer (IGV, Broad Institute, MA). The expression of *Myh6* was comparable in LV tissues after transduction with control RNAi (12,118 reads per million transcripts) and 403i RNAi (11,675 reads per million transcripts), indicating that the wild-type allele was not silenced *in vivo*. In contrast, the ratio of *Myh6* R403Q to *Myh6* (wild-type) reads varied between 403i RNAi titers. Only the highest titer (5×10^{13} vg/kg) resulted in a significant reduction (28.5 %) in the relative expression of *Myh6* R403Q compared to wild-type *Myh6* transcripts (P = 2.5E-5) (fig.S1c).

To assess the impact of silencing *Myh6* R403Q on HCM development, we injected virus encoding the 403i RNAi cassette (n= 8) or control RNAi cassette (n=7) into the thoracic cavity of one-day old male $MHC^{403/+}$ mice. At 5 to 6 weeks of age, all mice were given cyclosporine A (CsA) for 3 weeks to accelerate the emergence of HCM histopathology, as described(13). Mice were serially evaluated by echocardiography and at sacrifice, the hearts were analyzed by histopathology. After CsA treatment, control RNAi-transduced mice had LV hypertrophy and severe HCM histopathogy (Fig. 2A), similar to non-transduced, CsA-treated $MHC^{403/+}$ mice (13).

In contrast, CsA-treated $MHC^{403/+}$ mice transduced with 403i RNAi did not develop HCM (Table 1, upper panel). The left ventricular wall thickness (LVWT) of 403i RNAi-transduced mice (0.84 ± 0.10 mm) was significantly less than that of mice transduced with control RNAi (1.52 ± 0.25 mm, P = 1.9E-5) and comparable to the LVWT of wild-type mice (0.74 ± 0.05mm, NS) (12). Myocardial disarray (Fig. 2B) was absent and fibrosis (Fig. 2C) was significantly reduced in 403i RNAi-transduced mice (0.43 ± 0.11%) compared to control RNAi-transduced hypertrophic $MHC^{403/+}$ mice (2.12 ± 0.57%, P = 0.003). QRS interval prolongation, an electrocardiographic feature of LV hypertrophy, was present in mice transduced with control RNAi (20.5 ± 1.2 ms) but not in mice transduced with 403i RNAi (16.9 ± 1.4 ms, P = 0.001) (Fig. 2D). Additionally, the expression of prototypic LV hypertrophy markers *Nppa* and *Nppb* were 2.5 fold higher in mice transduced with control RNAi compared to 403i RNAi (Fig. 2E).

To assess if the early age at transduction and/or viral titer influenced HCM development, we injected high (5×10^{13} vg/kg) and low (5×10^{12} vg/kg) titer viruses of 403i RNAi in 3-week old $MHC^{403/+}$ mice (n=5). At 4 weeks, mice were treated with CsA for 3 additional weeks followed by echocardiography to assess LVWT and diastolic (relaxation) performance (left atrial diameter normalized to the aortic root diameter(20)) which becomes abnormal early in HCM (21) Mice transduced with high viral titers of control RNAi or low viral titers of 403i RNAi had both LV hypertrophy and diastolic dysfunction (Table 2). In contrast, mice transduced with high titer 403i RNAi virus had neither hypertrophy (LVWT= 0.72 ± 0.05 mm, P = 1.9E-6 compared to control RNAi) nor diastolic dysfunction (1.17 ± 0.09, P = 0.009 compared to control RNAi).

Using the high titer virus we next asked whether 403i RNAi-transduction could alter established HCM, by pretreating $MHC^{403/+}$ mice with CsA for 3 weeks to induce hypertrophy (LVWT, 1.40 ± 0.11 mm) prior to viral transduction. Echocardiography assessments at two months after 403i RNAi (n=3) transduction showed no change in LVWT (Table 1, middle panel), suggesting the treatment was ineffective in reversing established disease.

To determine whether 403i RNAi-transduction affected the pathologic LV remodeling that slowly emerges in $MHC^{403/+}$ mice with age in the absence of CsA, we monitored LV hypertrophy in mice transduced with a single high titer dose of 403i RNAi (n=5) or control RNAi (n=6) on day one of life. At 6 months, mice transduced with control RNAi had LV hypertrophy (LVWT, 0.93 ± 0.11 mm). There was no LV hypertrophy in mice transduced with 403i RNAi (LVWT= 0.68 ± 0.09 mm, P = 0.004) and LVWT was indistinguishable from wild-type mice (LVWT, 0.74 ± 0.05 mm, P = NS). Importantly, the protective effect of the 403i RNAi-vector dissipated over time. LV hypertrophy emerged in 403i RNAi-transduced mice by 11 months of age (LVWT, 0.87 ± 0.11 mm) and was comparable to that observed in control RNAi-transduced mice. The inadequacy to fully suppress hypertrophy in $MHC^{403/+}$ mice life-long is presumably due to diminished AAV-mediated transgene expression that occurs 7 months after transduction (22) and sub-therapeutic 403i RNAi levels.

Finally, we considered whether a single RNAi might silence different, patient-specific mutations in the same gene, by targeting a nearby single nucleotide polymorphism (SNP) that distinguished the mutant from wild-type alleles. To test this model, we produced male F1 offspring from 129SvEv $MHC^{403/+}$ and wild-type FVB crosses. We constructed an RNAi that targeted a 129SvEv SNP on the *Mhy6* allele (designated 129i, Fig. 1A) and transfected this with *Mhy6* R403Q (129SvEv) or wild-type *Myh6* (FVB) plasmids into 293T cells. The 129i RNAi decreased *Mhy6* R403Q levels by 75% and reduced wild-type *Myh6* (FVB) by only 15% (Fig. 1C). We produced AAV-9-cTnT-EGFP-129i virus and transduced (5×10^{13} vg/kg) one-day old male F1 $MHC^{403/+}$ mice with 129i RNAi (n= 4) or control RNAi (n=5). At 4 weeks of age, mice were treated with CsA for 2 weeks and studied by echocardiography. Control RNAi-transduced mice developed LV hypertrophy (LVWT=1.37 ± 0.03 mm) but not $MHC^{403/+}$ mice transduced with 129i RNAi (LVWT = 0.73 ± 0.07 mm; P = 1.6E-6, Table 1). We conclude from these studies that one RNAi construct which targeted a SNP that demarcates mutant and wild-type alleles could be used to silence distinct HCM mutations in a gene or to augment mutation-specific RNAi.

AAV-9 mediated RNAi preferentially suppresses the expression of the *Myh6* R403Q allele in a mouse model of HCM, by directly targeting the mutation or a nearby SNP. It is noteworthy that in a mouse model characterized by accelerated onset and severity of HCM, reduction in the expression levels of the mutant allele by only 28.5% (fig. 1Sc) was sufficient to abrogate hypertrophy and histopathologic remodeling for several months. Indeed, the LVWT in 403i-treated $MHC^{403/+}$ mice, with or without CsA, was comparable to that in wild-type mice. Based on these findings and evidence for unequal expression of mutated and wildtype *MYH7* mRNAs in human HCM hearts (23), we suggest that variable

penetrance and severity of HCM may reflect, at least in part, the proportion of wild-type and mutant transcripts and proteins.

The capacity for RNAi to attenuate expression of *Myh6* R403Q transcripts and abrogate HCM in mice raises the possibility that mutation silencing might benefit human cardiomyopathy patients. While our study provides proof-of-concept and does not address the many important potential problems associated with viral-mediated gene therapy (including the potential for immune response, and long-term off-target effects), some adeno-associated virus protocols are sufficiently safe for human clinical trials (24). Moreover, the potential to develop RNAi molecules that target allelic-specific, common SNPs rather than each patient's specific mutation, overcomes the daunting challenge of producing thousands of RNAi that would be required to silence each unique HCM or DCM mutation. There are also new opportunities to deliver gene silencing therapies to the heart. For example, the septal perforating artery can be selectively cannulated to target interventions to the interventricular septum (25), which in the majority of patients is the most profoundly hypertrophied segment in HCM heart and can cause obstruct ventricular outflow of blood, and increase the risk for sudden death. Adaptation of this approach could facilitate prophylactic, localized silencing of HCM mutations in this region where its benefit could be measurable and clinically meaningful. When continued advances in viral (and other) delivery systems (26, 27), allele-selective silencing holds considerable potential to retard the onset and progression of HCM and other genetic cardiomyopathies.

Supplementary Material

Refer to Web version on PubMed Central for supplementary material.

Acknowledgments

We thank Joshua Gorham, David Conner, and Steve DePalma for technical and bioinformatic assistance and Constance Cepko for assistance with viral protocols. This work was supported by grants from the NIH (U01HL098166; R01HL084553 to JGS and CES) and the Howard Hughes Medical Institute (CES).

References

1. Spirito P, Seidman CE, McKenna WJ, Maron BJ. The management of hypertrophic cardiomyopathy. N Engl J Med. 1997 Mar 13.336:775. [PubMed: 9052657]
2. Ho CY. Hypertrophic cardiomyopathy in 2012. Circulation. 2012 Mar 20.125:1432. [PubMed: 22431884]
3. Maron BJ, Maron MS. Hypertrophic cardiomyopathy. Lancet. 2013 Jan 19.381:242. [PubMed: 22874472]
4. Maron BJ, Doerer JJ, Haas TS, Tierney DM, Mueller FO. Sudden deaths in young competitive athletes: analysis of 1866 deaths in the United States, 1980–2006. Circulation. 2009 Mar 3.119:1085. [PubMed: 19221222]
5. Seidman JG, Seidman C. The genetic basis for cardiomyopathy: from mutation identification to mechanistic paradigms. Cell. 2001 Feb 23.104:557. [PubMed: 11239412]
6. Teekakirikul P, Padera RF, Seidman JG, Seidman CE. Hypertrophic cardiomyopathy: translating cellular cross talk into therapeutics. J Cell Biol. 2012 Oct 29.199:417. [PubMed: 23109667]
7. Lopes LR, Rahman MS, Elliott PM. A systematic review and meta-analysis of genotype-phenotype associations in patients with hypertrophic cardiomyopathy caused by sarcomeric protein mutations. Heart. 2013 May 14.

8. Geisterfer-Lowrance AA, et al. A molecular basis for familial hypertrophic cardiomyopathy: a beta cardiac myosin heavy chain gene missense mutation. Cell. 1990 Sep 7.62:999. [PubMed: 1975517]
9. Geisterfer-Lowrance AA, et al. A mouse model of familial hypertrophic cardiomyopathy. Science. 1996 May 3.272:731. [PubMed: 8614836]
10. Tyska MJ, et al. Single-molecule mechanics of R403Q cardiac myosin isolated from the mouse model of familial hypertrophic cardiomyopathy. Circ Res. 2000 Apr 14.86:737. [PubMed: 10764406]
11. Fatkin D, et al. An abnormal Ca(2+) response in mutant sarcomere protein-mediated familial hypertrophic cardiomyopathy. J Clin Invest. 2000 Dec.106:1351. [PubMed: 11104788]
12. Kim JB, et al. Polony multiplex analysis of gene expression (PMAGE) in mouse hypertrophic cardiomyopathy. Science. 2007 Jun 8.316:1481. [PubMed: 17556586]
13. Teekakirikul P, et al. Cardiac fibrosis in mice with hypertrophic cardiomyopathy is mediated by non-myocyte proliferation and requires Tgf-beta. J Clin Invest. 2010 Oct.120:3520. [PubMed: 20811150]
14. Semsarian C, et al. The L-type calcium channel inhibitor diltiazem prevents cardiomyopathy in a mouse model. J Clin Invest. 2002 Apr.109:1013. [PubMed: 11956238]
15. Jones WK, et al. Ablation of the murine alpha myosin heavy chain gene leads to dosage effects and functional deficits in the heart. J Clin Invest. 1996 Oct 15.98:1906. [PubMed: 8878443]
16. de Fougerolles A, Vornlocher HP, Maraganore J, Lieberman J. Interfering with disease: a progress report on siRNA-based therapeutics. Nat Rev Drug Discov. 2007 Jun.6:443. [PubMed: 17541417]
17. Gao G, Vandenberghe LH, Wilson JM. New recombinant serotypes of AAV vectors. Curr Gene Ther. 2005 Jun.5:285. [PubMed: 15975006]
18. Prasad KM, Xu Y, Yang Z, Acton ST, French BA. Robust cardiomyocyte-specific gene expression following systemic injection of AAV: in vivo gene delivery follows a Poisson distribution. Gene Ther. 2011 Jan.18:43. [PubMed: 20703310]
19. Christodoulou DC, Gorham JM, Herman DS, Seidman JG. Construction of normalized RNA-seq libraries for next-generation sequencing using the crab duplex-specific nuclease. Curr Protoc Mol Biol. 2011 Apr.4(4):12. [PubMed: 21472699]
20. Lang RM, et al. Recommendations for chamber quantification: a report from the American Society of Echocardiography's Guidelines and Standards Committee and the Chamber Quantification Writing Group, developed in conjunction with the European Association of Echocardiography, a branch of the European Society of Cardiology. J Am Soc Echocardiogr. 2005 Dec.18:1440. [PubMed: 16376782]
21. Ho CY, et al. Assessment of diastolic function with Doppler tissue imaging to predict genotype in preclinical hypertrophic cardiomyopathy. Circulation. 2002 Jun 25.105:2992. [PubMed: 12081993]
22. Bish LT, et al. Adeno-associated virus (AAV) serotype 9 provides global cardiac gene transfer superior to AAV1, AAV6, AAV7, and AAV8 in the mouse and rat. Hum Gene Ther. 2008 Dec. 19:1359. [PubMed: 18795839]
23. Tripathi S, et al. Unequal allelic expression of wild-type and mutated beta-myosin in familial hypertrophic cardiomyopathy. Basic Res Cardiol. 2011 Nov.106:1041. [PubMed: 21769673]
24. Mingozzi F, High KA. Therapeutic in vivo gene transfer for genetic disease using AAV: progress and challenges. Nat Rev Genet. 2011 May.12:341. [PubMed: 21499295]
25. Elmariah S, Fifer MA. Medical, surgical and interventional management of hypertrophic cardiomyopathy with obstruction. Curr Treat Options Cardiovasc Med. 2012 Dec.14:665. [PubMed: 22956194]
26. Rodriguez-Lebron E, Paulson HL. Allele-specific RNA interference for neurological disease. Gene Ther. 2006 Mar.13:576. [PubMed: 16355113]
27. Yu D, et al. Single-stranded RNAs use RNAi to potently and allele-selectively inhibit mutant huntingtin expression. Cell. 2012 Aug 31.150:895. [PubMed: 22939619]

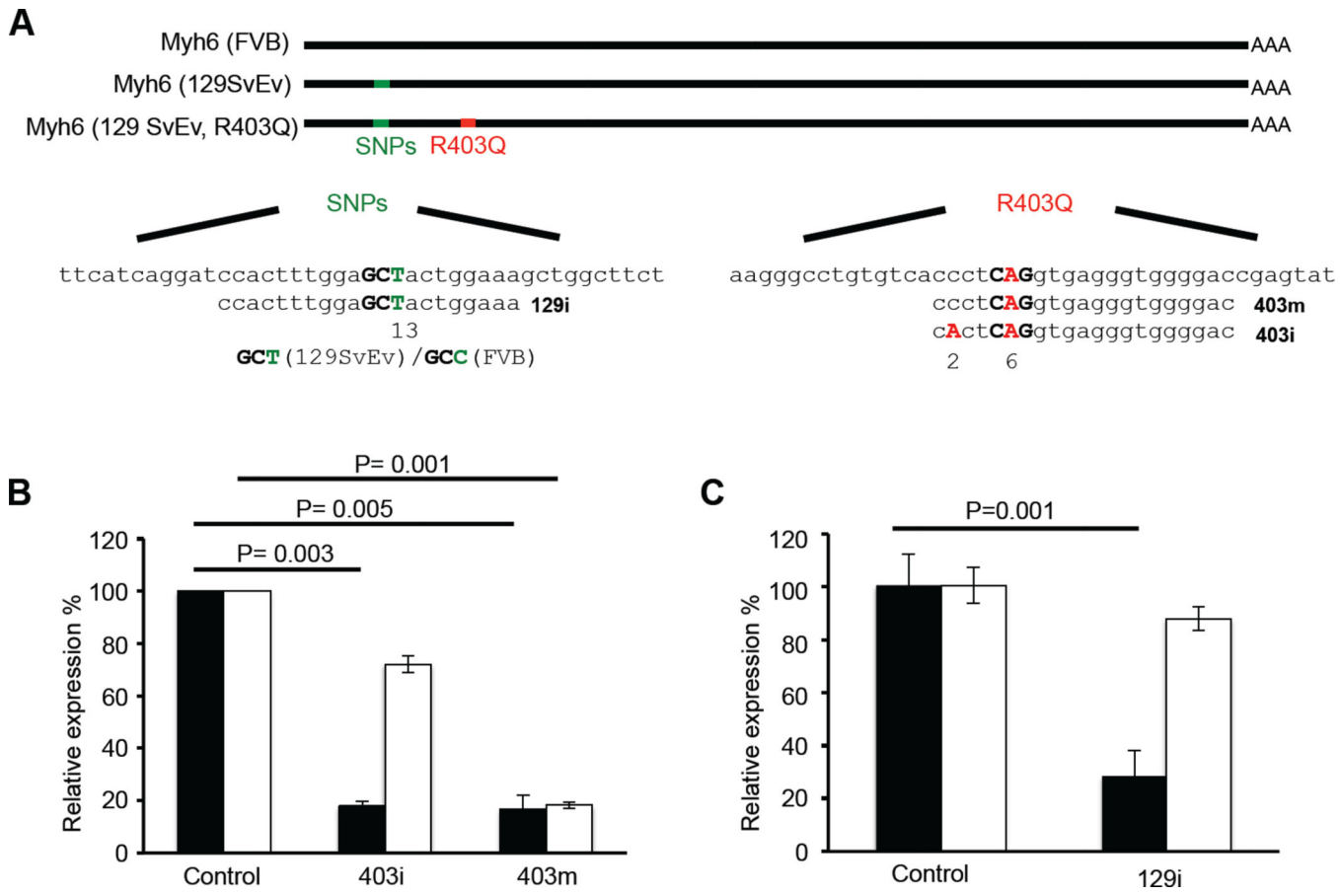

Fig. 1. Selective silencing of *Myh6* R403Q expression by AAV-9-mediated RNAi

(A) Schematic representation of FVB, 129SvEv, 129SvEv mutant (R403Q) transcript and RNAi sequences. (B) Quantitative real-time PCR analysis of wild-type *Myh6* (white bar) and mutant *Myh6* R403Q (black bar) expression after transduction of the 403m and 403i constructs (n=4). Levels of the transcripts were normalized to control LacZ RNAi. (C) Quantitative real-time PCR analysis of FVB *Myh6* (white bar) and 129SvEv *Myh6* R403Q (black bar) expression after transduction of the 129i construct (n=4). Levels of the transcripts were normalized to control LacZ RNAi. Data are presented as the mean ± s.d.

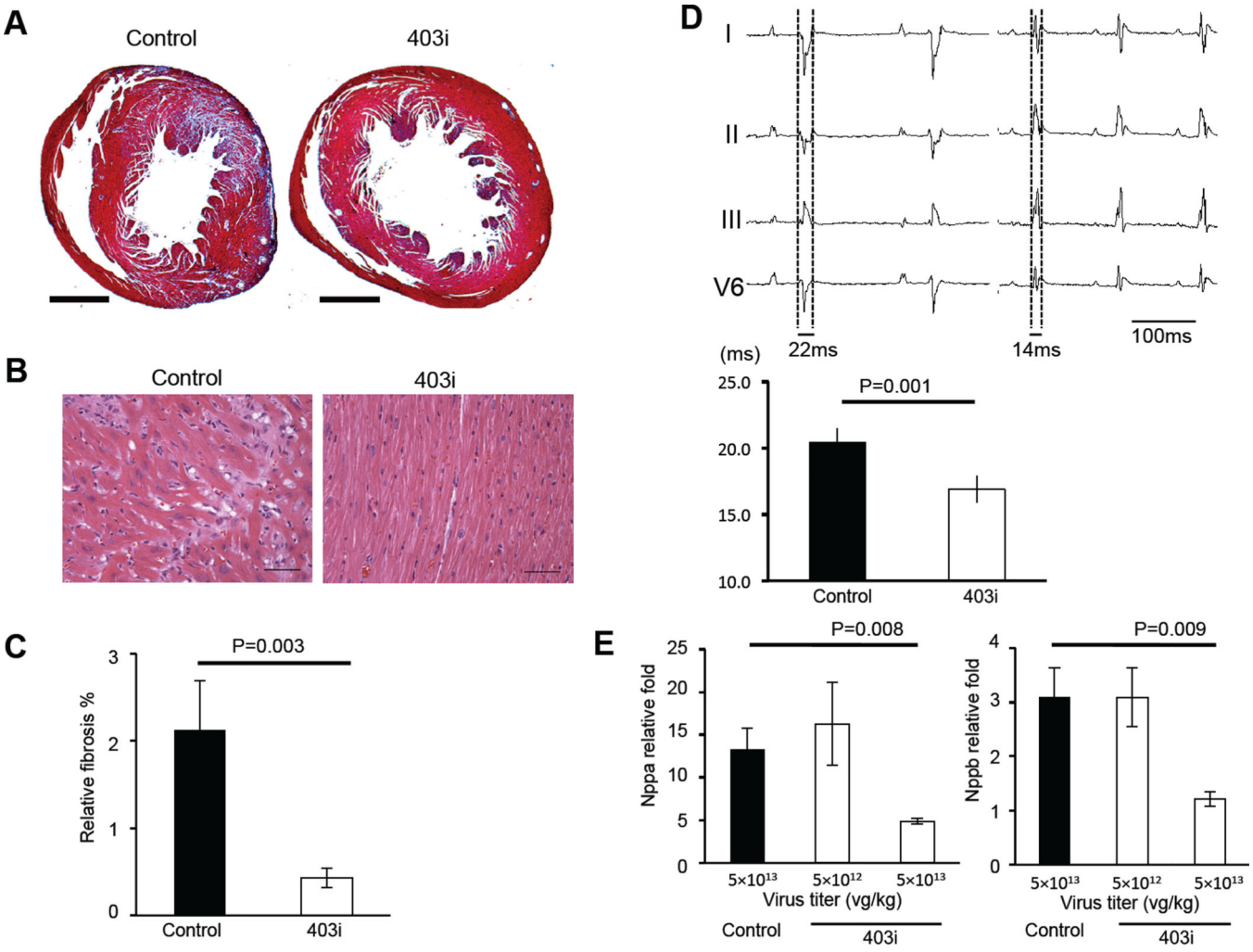

Fig. 2. *In vivo* effect of *Myh6* R403Q silencing

(A) Cardiac histopathology from MHC$^{403/+}$ mice transduced with control RNAi (left) and 403i RNAi (right). Masson trichrome staining reveals marked fibrosis (blue) in MHC$^{403/+}$ mice transduced with control RNAi. Bar =1 mm. (B) Hematoxylin and eosin staining shows myocyte disarray in MHC$^{403/+}$ mice transduced with control RNAi (left) and normal myocyte architecture in mice transduced with 403i RNAi (right). Bar = 100 μm. (C) Quantification of myocardial fibrosis in MHC$^{403/+}$ mice transduced with control RNAi (black bar, n=4) and 403i RNAi (white bar, n=4). (D) An electrocardiogram of MHC$^{403/+}$ mice transduced with control RNAi (left top panel) and 403i RNAi (right top panel). Mice transduced with control RNAi have prolonged QRS (ventricular conduction) interval and high voltage P waves consistent with LV hypertrophy and atrial enlargement. The bottom panel presents QRS intervals from mice transduce with control RNAi (black bar, n=5) and 403i RNAi (white bar, n=6). (E) Quantitative real-time PCR analysis of *Nppa* (left panel) and *Nppb* (right panel) expression after transduction of control RNAi (black bar) and two different doses of 403i constructs (white bar) (n=5). Levels of the transcripts were

normalized to transcript levels from age matched wild-type hearts. Data are presented as the mean ± s.d.

Table 1

RNAi effects on cardiac morphology and function in HCM mice. To accelerate hypertrophic remodeling in $MHC^{403/+}$ mice CsA was administered for the number of weeks indicated either after (Post) RNAi transduction on day 1 or for 3 weeks prior (Pre) to RNAi transduction on day 21. No CsA denotes $MHC^{403/+}$ mice not treated with CsA. Age, denotes age at time of cardiac evaluation; (#) number of mice studies. LVDD, LV diastolic dimensions; LVWT, LV wall thickness; FS, percent fractional shortening. Cardiac dimensions and function with associated P values, calculated by T-test, reflect comparisons to $MHC^{403/+}$ transduced with control RNAi. Values for wildtype 129SvEv mice, not treated with CsA, are shown for comparison. Data are presented as the mean ± s.d

CsA	RNAi	Age (#)	LVDD	P value	LVWT	P value	FS (%)	P value
3 weeks, Post	Control	8 weeks (n=7)	2.53 ± 0.41		1.52 ± 0.25		32.68 ± 6.68	
	403i	8 weeks (n=8)	3.04 ± 0.21	0.01	0.84 ±0.10	1.90E-05	40.37 ± 5.39	0.04
3 weeks, Pre	None	6 weeks (n=3)	2.92 ± 0.28		1.40 ± 0.11		28.38 ± 5.16	
	403i	14 weeks (n=3)	3.50 ± 0.16	NS	1.42 ± 0.06	NS	30.61 ± 4.59	NS
No CsA	Control	6 months (n=6)	3.54 ± 0.27		0.93 ± 0.11		33.30 ± 4.02	
	403i	6 months (n=5)	3.75 ± 0.21	NS	0.68 ±0.09	0.005	33.42 ± 7.61	NS
	Control	11 months (n=6)	3.66± 0.25		0.98 ± 0.16		37.8 ± 11.11	
	403i	11 months (n=5)	3.93 ± 0.48	NS	0.87 ± 0.11	NS	36.11± 8.86	NS
2 weeks, Post	Control	6 weeks (n=5)	2.62± 0.20		1.37 ± 0.07		33.75 ± 4.51	
	129i	6 weeks (n=4)	3.85 ± 0.22	0.001	0.73 ± 0.03	1.60E-06	28.21 ± 9.34	NS
WT, no CsA	None	6 months (n=4)	3.75 ± 0.28		0.74 ± 0.05		30.01 ± 3.73	

Table 2

Viral dosage need for RNAi effects on cardiac morphology and function in HCM mice. $MHC^{403/+}$ mice (n= number) were transduced with RNAi at vector genomes per kg (titer) per kg on day 1 and treated with CsA for 3 weeks to accelerate hypertrophic remodeling. LVDD (LV diastolic dimension; LVWT, LV wall thickness; FS%, percent fractional shortening and left atria (LA) dimension normalized to the aortic root (Ao) are provide. Cardiac dimensions and function with associated P values, calculated by T-test, reflect comparisons to $MHC^{403/+}$ transduced with control RNAi. Data are presented as the mean ± s.d

RNAi	titer	LVDD (mm)	P value	LVWT (mm)	P value	FS (%)	P value	LA/Ao root	P value
Control (n=5)	5×10^{13}	3.18 ± 0.24		1.34 ± 0.09		31.18 ± 7.27		1.46 ± 0.12	
403i (n=5)	5×10^{13}	3.33 ± 0.15	NS	0.72 ± 0.05	1.9E-6	38.09 ± 4.64	NS	1.17 ± 0.09	0.009
403i (n=5)	5×10^{12}	3.06 ± 0.34	NS	1.26 ± 0.26		30.33 ± 3.64		1.39 ± 0.12	